# Mathematical Modeling of Geo-thermo-mechanical Processes in Lithospheric-asthenospheric Subduction Systems using Numerical Methods

Sergey Gavrilov and Andrey Kharitonov

*Abstract* - **The purpose of work is to develop a numerical method for mathematical modeling geo-thermo-mechanical processes in lithosphere-asthenospheric subduction systems, which is used to predict the geographical location of deposits of rare, non-ferrous, ferrous metals. Here are given the results of anomalous heat flux distribution analysis in the back-arc part of subduction zone at the Pakistani territory, where the heat flux anomaly is by ~ 9% less than that at the western portion of this zone, despite the subduction velocity of Arabian plate, on the contrary, is 1.48 times greater (subduction angle is somewhat less) at the Pakistani block of subduction zone. The model of dissipative heating and convective dissipative heat transfer to the Earth's surface computed with taking account of the non-Newtonian mantle rheology and phase transitions shows the water content to be by 0.54 weight % greater and activational energy by 40 (kJ/mol) less in the Pakistani mantle wedge portion as compared to the Iranian one, the maximum heat flux anomaly being shifted by ~$10^2$ km further landward from the deep-sea trench. The results of modeling of the geo-thermo-mechanical processes in the mantle wedge at the subduction zone show the copper-porphyry ore deposits to possibly be found there.**

*Keywords* - **lithosphere-asthenospheric subduction systems, mathematical modeling, numerical method, prospecting.**

## I. Introduction

In [1], [2], [3] an opinion of some foreign specialists is put forward that in the investigations of metal genesis there exist a number of unresolved theoretical and practical problems linked with the search of new deposits of rare, non-ferrous and ferrous metals. In particular, the causes of origin of metal provinces of certain geochemical composition are thus far debated, especially so far as some geographical regions of the Earth's surface (including Eurasia) are concerned. To clarify the existing problem peculiarities in details it is necessary to explain that according to [3] the entire Earth's surface is subdivided into 6 global and the number of smaller lithospheric plates. Subduction zones are as a rule localized at the boundaries between oceanic and continental plates, which zones are in our opinion the basic geological-tectonic regions where the metal provinces are formed by definite geo-thermo-mechanical processes. Zones of lithospheric subduction usually are the ones of collision of lithospheric plates where the relatively cold oceanic plates are thrust under continental ones and gradually (however usually in a stick-slip regime) sink into the mantle. Here we attempt to explain the origin, geographical distribution and causes of formation of certain kind of ores in metal provinces from the viewpoint of global plate tectonics [1], [2], [3]. One of the typical subduction regions is the Arabian – Eurasian zone of subduction of lithosphere plates (AEZSLP). As an example of application of new numerical approach to prospecting new metal provinces worked out by the authors on the basis of analysis of geo-thermo-mechanical processes in mantle wedges, regional geological and geophysical investigations were carried out in the Arabian – Eurasian subduction zone. The results of these investigations show considerable deposits of minerals to possibly be found in this region. In Fig. 1 the generalized scheme of the region under investigation is outlined, which serves as an example of application of numerical method of prospecting the geographical location of metal provinces.

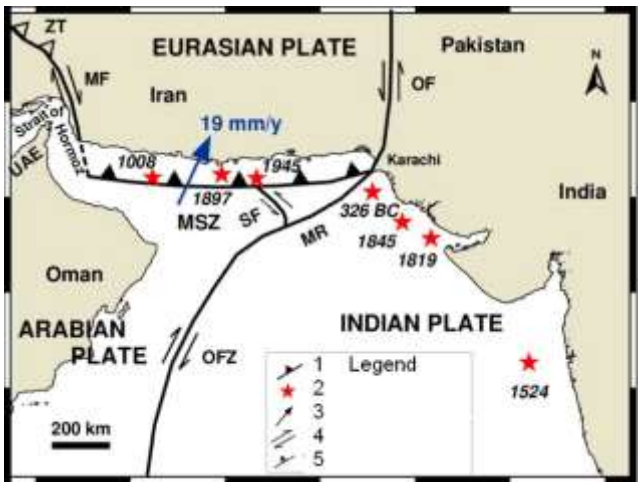


Fig. 1 Outline of the region of investigation in the northern (rear) part of the zone of lithospheric subduction of Arabian suboceanic plate under Eurasian continental lithosphere plate (Arabian-Eurasian (Makran) subduction zone) [4]. Legend: 1 – Makran subduction zone (MSZ) at the continental Eurasian plate; 2 – locations of the earthquake epicenters and tsunami event; 3 – direction of motion and velocity (19 mm/y) of Arabian suboceanic plate subducting under Eurasian continental lithosphere plate; 4 – strike slip fault; 5 – thrust faults in the southern territory of Eurasian plate and Arabian plate (MF- Minab fault, MR – Murray ridge, OF – Ornah-Nal fault, OFZ – Owen fracture zone, SF – Sonne fault, ZT – Zagroz thrast).

## II. Used data

To carry out the geo-thermo-mechanical investigations at the Arabian-Eurasian zone of subduction of lithospheric plates (AEZSLP) here we made use of the data of the digital heat flux data bank [5] and the satellite map of gravity field

[6]. These were used to solve direct and inverse problems of determining the deep structure and geo-thermo-mechanical parameters of rocks at AEZSLP. In [7] the two 2D zones of anomalously enlarged surface heat flux are reported to locate in the near-to-shore tectonic zone parallel to AEZSLP (Fig. 2).

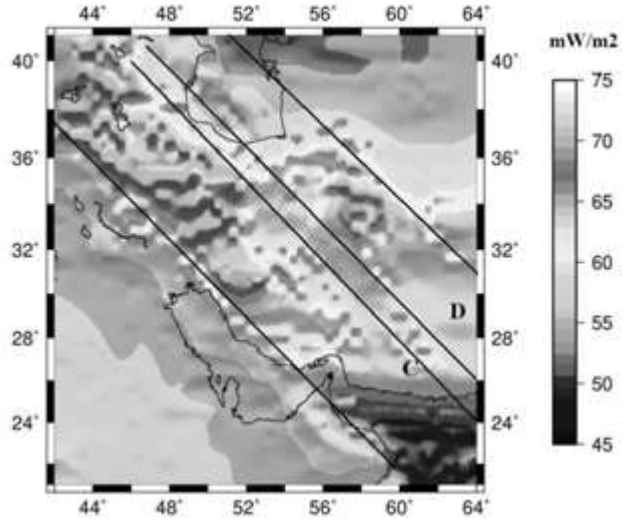


Fig. 2 The map of two basic linear zones (C and D) of anomalously enlarged surface heat flux generated by geo-thermo-mechanical processes in AEZSLP [5], [7].

In the post-Proterozoic period of the Earth's evolutionary transformation upwelling convective flows transported to the upper crustal layers the lime-alkali melts containing ores of different chemical composition. In [5], [7] the enlarged surface heat flux anomalies are noted to allow presuming convective Karig's vortices to exist in the interiors of the Earth's mantle with a possible presence of plutonic intrusions of ore deposits in the upper layers of the Earth's crust locating above Karig's vortices.

## III. Numerical modelling of geo-thermo-mechanical processes (dissipative heat generation, viscosity, and pore water content) in mantle wedge rocks within the AEZSLP region

The present study outlines a multi-stage numerical methodology for identifying the spatial distribution of metalliferous provinces andelucidating the geochemical composition of their ore deposits. The computational procedure comprises the following sequential steps:

### *A. Parameterisation of geo-thermo-mechanical processes in the AEZSLP mantle wedge*

Utilising empirical data on surface heat flux [5] and supplementary geophysical parameters of the mantle, we computed key characteristics of sub-mantle dynamics. This yielded quantitative estimates of: $h_u$ and $h_b$ depths of the upper and lower boundaries of heterogeneities linked to convective mantle wedge vortices; $F$ – morphological configuration of heterogeneities; $L$ – horizontal extent of anomalous structures.

### *B. Determination of subduction angle (β)*

Seismological data on hypocenter distribution enabled calculation of the Arabian lithospheric plate's subduction angle ($\beta$).

### *C. Density estimation (ρ) of rocks in convective vortices*

An invers problem was solved using gravity field data [6], incorporating previously derived geometrical parameters ($h_u, h_b, F, L$) of convective structures within the AEZSLP tectonic zone. Based on established rock density ($\rho$) and convective vortex depth, inferences were drawn regarding the geochemical composition of metallic fractions in ore deposits situated above single or multiple convective vortices.

### *D. Detailed methodology for characterising geo-thermo-mechanical processes in the AEZSLP mantle wedge*

We simulate the thermo-mechanical state of the mantle wedge in the western subduction zone segment, where aseismic subduction prevails. The novelty of our approach lies in the initial assumption of non-Newtonian rheology for the mantle wedge medium. This is justified by elevated water content - expelled from the subducting slab – which significantly reduces effective viscosity and promotes dislocation creep as the dominant deformation mechanism. A further distinguishing feature of the model is the prioriti sation of dissipative heating in the AEZSLP mantle wedge before simulating convective heat transfer to the Earth's surface. This allows assessment of how subduction regime (aseismic vs. stick-slip) influences surface heat flux anomalies via dissipative heat release intensity.

### *E. Mathematical formulation*

The thermo-mechanical model of the mantle wedge – situated between the base of the overlying Eurasian continental lithosphere (encompassing the rear zone of the western AEZSLP lithospheric block) and the upper surface of the suboceanic Arabian lithospheric plate (subducting beneath the Iranian coast at velocity $V$ and angle $\beta$) – is derived from dimensionless 2D hydrodynamic equations for stream function $\psi$ and temperature $T$ [8]:

$$(\partial^2_{zz} - \partial^2_{xx})\eta(\partial^2_{zz} - \partial^2_{xx})\psi + 4\partial^2_{xz}\eta\partial^2_{xz}\psi = RaT_x - Ra^{(410)}\Gamma_x^{(410)} - Ra^{(660)}\Gamma_x^{(660)}, \quad (1)$$

$$\partial_t T = \Delta T - \psi_z T_x + \psi_x T_z + (Di/Ra)\times(\tau_{ik}^2/2\eta) + Q. \quad (2)$$

$\eta$ – dynamic viscosity;

$\partial$ with subscripts – partial derivatives with respect to $x$ (horizontal), $z$ (vertical), and $t$ (time);

$\Delta$ – Laplace operator;

$I^{(410)}$ and $I^{(660)}$) – volume fractions of the dense phase at 410 km and 660 km phase boundaries;

$V_x$ and $V_z$ – horizontal and vertical velocity components, expressed via $\psi$ as:

$$V_x = \psi_z,\ V_z = -\psi_x, \quad (3)$$

***F. Dimensionless parameters***:

Rayleigh number: $Ra = \alpha\rho g d^3 T_1/(\eta\chi) = 5.55\times10^8$; (4a)

Phase-specific Rayleigh numbers:

$$Ra^{(410)} = \delta\rho^{(410)} g d^3/(\eta\chi) = 6.6\times10^8; \quad (4b)$$

$$Ra^{(660)} = \delta\rho^{(660)} g d^3/(\eta\chi) = 8.5\times10^8; \quad (4c)$$

Dissipative number: $Di = \alpha\rho g/c_p = 0.165$. (4d)

- $\alpha = 3\times10^{-5}$ ($K^{-1}$) – thermal expansion coefficient;
- $\rho = 3.3\times10^3$ ($kg/m^3$) – density;
- $g$ – gravitational acceleration;
- $c_p = 1.2\times10^3$ J/(kg· K) – specific heat at constant pressure;
- $T_1$ = 1950ºK – temperature at MTZ base (660 km depth);
- $Q = 6.25\times10^{-4}$ ($mW/m^3$) – volumetric crustal heat generation;
- $\tau_{ik}$ – viscous stress tensor;
- $d$ = 660 km – vertical domain extent;
- $\eta = 10^{18}$ (Pa · s) – viscosity scaling factor;
- $\chi = 1$ ($mm^2/s$) – thermal diffusivity;
- $\delta\rho^{(410)} = 0.07\rho$, $\delta\rho^{(660)} = 0.09\rho$ – density jumps at 410 km and 660 km.

Scaling factors for $t$, $x$, $z$, $\tau_{ik}$, and $\psi$ are $(d^2/\chi)$, $(\eta\chi/d^2)$, and $\chi$, respectively.

***G. Viscosity model***

Unlike [9], which assumes Newtonian rheology and diffusion creep dominance below ~ 200 km, our model accounts for dislocation creep prevalence in mantle wedges due to high water content from slab dehydration. Consequently, viscosity ($\eta$) depends on:

$C_w$ – water concentration;

$\tau_{ik}$ – viscous stress tensor;

$T$ – temperature;

$p$ – lithostatic pressure.

***H. The viscosity formulation is***:

$$\eta = (2AC_w^r \tau^{n-1})^{-1} \times (h/b^*)^m \times \exp[(E^* + pV^*)/(RT)], \quad (5)$$

where for «wet» olivine [10]: $n = 3$, $r = 1.2$, $m = 0$, $\tau = (\tau_{ik}^2)^{1/2}$, $E^* = 480$ (kJ/mol), $V^* = 11\times10^3$ ($mm^3$/mol), $A=10^2$($s^{-1}$·$(MPa)^{-n}$), $C_w > 10^{-3}$ (wt. %).

For $C_w = 10^{-3}$ wt. %, and given:

$$\tau_{ik}^2 = 4\eta^2[(\psi_{zz} - \psi_{xx})^2/2 + 2\psi_{xz}^2], \quad (6)$$

The dimensionless viscosity ($\eta$) is defined by the following expression:

$$\eta = [(½\cdot(\psi_{zz} - \psi_{xx})^2 + 2\psi_{xz}^2]^{-1/3} \times \exp\{[10.0 + 5.0(1 - z)]/T\}. \quad (7)$$

where:

$T$ – denotes the dimensionless temperature;

$z$ – represents the dimensionless vertical coordinate (normalized with respect to $d$ = 650 km), measured upward from the base of the mantle transition zone (MTZ);

$x$ – axis is oriented opposite to the direction of subduction along the lower boundary of the MTZ.

The computational domain in the AEZSLP region adopts an aspect ratio of 1:2.25. Under diagonal subduction conditions, this corresponds to a subduction angle $\beta = 24$º. The empirically observed subduction velocity in the Iranian segment is $V$=19mm/yr. When expressed in dimensionless form via $(\chi/d)$, this yields $V = 0.416\times10^3$. Consequently, within the Arabian lithospheric plate subducting beneath the Iranian AEZSLP segment, the dimensionless velocity components are:

$V_x = -0.380\times10^3$,

$V_z = -0.170\times10^3$.

It is important to note that (7) assumes a water content $C_w = 10^{-3}$ wt. %. However, in the present model, we adopt $C_w$= 1 wt. %, which results in a reduction of the dimensionless viscosity by a factor of 3981 (i.e., $10^{3,6}$) compared to the reference case in (7). According to reference [11], the phase functions $\Gamma^{(l)}$ are formulated as follows (with the $z$-axis directed upward, necessitating sign adjustments):

$$\Gamma^{(l)} = ½ \times\{1 - \mathrm{th}[(z - z^{(l)}(T))/w^{(l)}]\}; \quad (8a)$$

$$z^{(l)}(T) = z_0^{(l)} - \gamma^{(l)}[T - T_0^{(l)}]/\rho g, \quad (8b)$$

where:

$z^{(l)}(T)$ is the depth of the $l$-th phase transition ($l$= 410, 660);

$z_0^{(l)}$ and $T_0^{(l)}$ denote the mean depth and temperature of the $l$-th phase transition;

$\gamma^{(410)} = 3$ (MPa/K) and $\gamma^{(660)} = -3$ (MPa/K) represent the slopes of the phase equilibrium curves;

$w^{(l)}$ is the characteristic thickness of the $l$-th phase transition;

$T_0^{(410)} = 1800$ºK and $T_0^{(660)} = 1950$ºK are the reference phase transition temperatures.

In the context of (2), the latent heats of phase transitions in the AEZSLP are considered negligible due to their minor influence on finite-amplitude convection, as discussed in [11]. From (8), the spatial derivative $\Gamma_x^{(l)}$ is derived as:

$\Gamma_x^{(l)} = -\frac{1}{2}\,(\gamma^{(l)}/\rho g w^{(l)}) \times \mathrm{ch}^{-2}\{[z - z_0^{(l)} + \gamma^{(l)}(T - T_0^{(l)})/(\rho g)]/w^{(l)}\} \times T_x,$ (9)

This formulation reveals that:

- a phase transition with $\gamma^{(l)} > 0$ (at $l$ = 410 km) enhances convective motion;

- a phase transition with $\gamma^{(l)} < 0$ (at $l$ = 660 km) inhibits convection.

In dimensionless units, the parameters are specified as:

- $z_0^{(410)} = 0.38, z_0^{(660)} = 0$;
- $w(l) = 0.05$;
- $\gamma^{(410)} = 2.55\times10^9, \gamma^{(660)} = -2.55\times10^9$;
- $T_0^{(410)} = 0.92, T_0^{(660)} = 1$.

Equation (10) generalizes $\Gamma_x^{(l)}$ in dimensionless form:

$\Gamma_x^{(l)} = -\frac{1}{2}\,\delta\rho^{(l)}\,\gamma^{(l)}/(\rho Ra^{(l)} w^{(l)}) \times \mathrm{ch}^{-2}\{[z - z_0^{(l)} + \gamma^{(l)}\,\delta\rho^{(l)}\,(T - T_0^{(l)})/\rho Ra^{(l)}]/w^{(l)}\} \times T_x$ (10)

Equations (1)–(2) are numerically solved under the assumption of isothermal, no-slip, impermeable horizontal and vertical boundaries – except at designated "windows" for the incoming and outgoing subducting plate, where velocity is prescribed. The lateral boundary distant from the subduction zone is treated as permeable at a right angle. This boundary condition is justified for cases of relatively shallow subduction geometry. The heat production term $Q$ in (2) is non-zero within the continental and oceanic crust, with thicknesses of 40 km and 7 km, respectively. The initial temperature profile at vertical boundaries is computed using a half-space cooling model over time spans of $10^9$ yr (Eurasian continental plate) and $10^8$ yr (Arabian suboceanic plate). Within the thermo-mechanical framework of the AEZSLP model, we compute the spatial distribution of volumetric dissipative heating, expressed as $[(1/2)\times(\tau_{ik})^2 \times \eta^{-1}]$. According to (6), its dimensionless form is:

$W_{diss} = \frac{1}{2}\,(\tau_{ik})^2 \times \eta^{-1} = 2\eta \times [\,\frac{1}{2}\,(\psi_{zz} - \psi_{xx})^2 + 2(\psi_{xz})^2]$,(11)

To convert this to dimensional form, the following scaling factor must be applied:

$(\eta\,\chi \cdot d^{-2})^2 \times \eta^{-1} = 0.53\times10^{-14}\,(\mathrm{mW/m^3})$, (12)

by which the dimensionless $W_{\mathrm{diss}}$ (11) is multiplied.

### IV. Comparative characteristics of mantle wedges in the western and eastern segments of AEZSLP

The results of numerical modeling of the quasi steady-state geo-thermo-mechanical state of upper mantle in the mantle wedge at the western segment of AEZSLP are presented in Fig. 3.

The equations (1) – (2) were integrated in time by the 3-rd order Runge-Kutta method on the grid of 104×104 size in space domain. In Fig. 3 (1) – (2) the steady-state non-dimensional temperature and stream-function are shown, found as a solution of (1) – (2) without accounting for convective instability and viscous dissipation. Rectilinear diagonal streamlines in Fig. 3(2) correspond to the subducting Arabian lithosphere plate. In Fig. 3(3) the arrows (1), (2), (3) indicate the non-dimensional volumetric dissipative heat release power $W_{diss}$ in the mantle wedge shown by isolines.

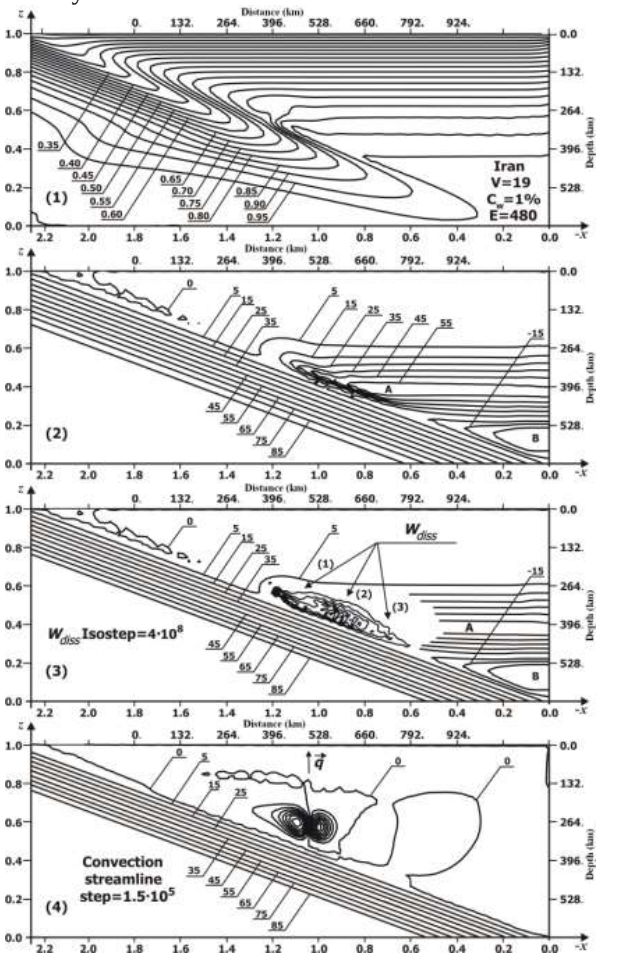


Fig. 3 presents the following computational results in a systematic arrangement:

(1) The steady-state profile of the dimensionless temperature field within the western sector of the mantle wedge associated with the AEZSLP, excluding the contributions of viscous dissipation and convective processes. Isothermal contours are rendered at intervals of 0,05 units.

(2) The equilibrium configuration of the dimensionless unperturbed stream function in the mantle wedge overlying the subducting Arabian lithospheric plate, disregarding viscous dissipation and convection effects. Streamlines are plotted with a spacing of 5 units. Diagonally oriented equidistant streamlines correspond to the kinematics of the rigidly subducting plate. The induced flow patterns labeled (A) and (B) are primarily driven by the subducting slab, with partial contribution from convective mechanisms. Spatial coordinates are measured in the meridional direction relative to the «edge corner» of the mantle wedge at latitude 29°N.

(3) The steady-state distribution of the dimensionless stream function in the western segment of the AEZSLP mantle wedge, superimposed with the spatial distribution of volumetric dissipative heat generation rate ($W_{diss}$). The latter is visualized through directional arrows marked (1), (2), and (3).

(4) The steady-state pattern of the dimensionless stream function within the western portion of the AEZSLP mantle wedge, incorporating the effects of developed convective motion. The vector $\boldsymbol{q}$ delineates the region of anomalous thermal flux transported via convection from the zone of maximal dissipative heat production ($W_{diss}$) toward the Earth's surface.

Heat release is concentrated in the zone of friction between the subducting slab and induced counter flow (A) in Fig. 3(2). This zone of the thickness of $\Delta d \sim 10^2$ km with the maximum non-dimensional heat release of $\sim 9\times10^9$ (with the dimensional $W_{diss\ max} \sim 5\times10^{-4}$ (mW/m$^3$) according to (12)) yields roughly the surface anomalous heat flux estimation of $\Delta q = \Delta d \times W_{diss\ max}$, i.e. $\Delta q \sim 50$ (mW/m$^2$) (without convective heat transfer), which value is or the order of the observed heat flux.

In Fig. 3(4) the quasi-steady-state non-dimensional stream-function is shown for convection taking place with a velocity of ~ 1 (m/yr) which channelizes heat transfer from the zone of maximum dissipative heat release to the zone of maximum surface heat flux shown by vector $\boldsymbol{q}$ at a distance of ~ 500 km from the deep-sea trench in the western segment of AEZSLP. There the parallel to the trench 2D zone of enlarged surface heat flux is actually observed in the western segment of AEZSLP territory.

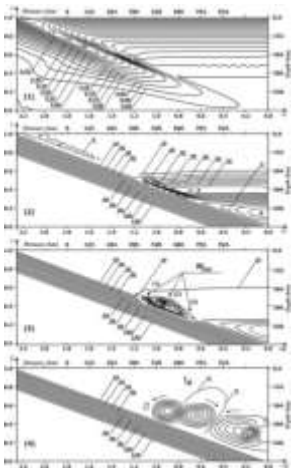

Fig. 4 presents the following computational results:

(1) The steady-state dimensionless temperature distribution within the eastern (Pakistani) segment of the mantle wedge associated with the AEZSLP, neglecting the contributions of viscous dissipation and convective processes. Isotherms are plotted at intervals of 0.05.

(2) The steady-state dimensionless unperturbed stream-function distribution in the mantle wedge overlying the subducting Arabian lithospheric plate, excluding the effects of viscous dissipation and convection. Streamlines are displayed with a spacing of 5 units. Diagonally arranged equidistant streamlines correspond to the rigid subducting plate. The induced flow patterns labeled (A) and (B) are primarily driven by the subducting slab, with partial contribution from convective mechanisms. Distance measurements are referenced along the meridional direction from the «edge corner» of the mantle wedge at 29°N.

(3) The steady-state dimensionless stream-function distribution in the western sector of the AEZSLP mantle wedge, superimposed with the volumetric dissipative heat release rate $W_{diss}$. The latter is visualized via directional arrows marked as (1), (2), and (3).

(4) The steady-state dimensionless stream-function distribution in the western portion of the AEZSLP mantle wedge, incorporating the influence of developed convective processes. The vector $q$ denotes the region of anomalous heat flux transported via convection from the zone of maximal dissipative heat generation ($W_{diss}$) toward the Earth's surface.

In the eastern segment of AEZSLP the subduction velocity equals 32.6 (mm/yr) (where the non-dimensional components of the Arabian lithospheric plate subduction velocity are $V_x = -0.620\cdot10^3$ and $V_z = -0.280\cdot10^3$), the angle of subduction is somewhat less but approximately the same as in the western segment of subduction zone.

For the activation energy $E^* = 440$ (kJ/mol) and $C_w = 1.48$ weight % in (7), the solution of (1) – (2) yields the model distribution of thermo-mechanical upper mantle parameters in the Pakistani segment of mantle wedge presented in Fig. 4. Extra water content in the Pakistani segment of mantle wedge may be thought to originate due to subducting slab being "shaken" by the earthquakes. As a consequence, water concentration $C_w$ increases and activational energy $E^*$ drops.

The dissipative heat release power and corresponding surface heat flux in the rear of eastern segment of subduction zone are by ~ 5–10% less than those in the rear of western segment, the geographical location of mantle heterogeneity linked with the convective heat flux transporting dissipative heat from the AEZSLP mantle wedge to the Earth's surface being clearly shifted by ~ $10^2$ km further landward from the trench as compared to Fig.3.

## V. Results and Discussion

In constructing the geo-thermo-mechanical model of mantle wedge medium between the overlying Eurasian continental lithosphere plate and subducting Arabian one it is first necessary to put in (1)–(2) $Ra \to 0$, $Di = 0$, i.e. to compute the model of subducting Arabian lithosphere plate, mantle wedge, and Eurasian lithosphere plate with no account taken of viscous dissipation and convection. Fig. 3(2) demonstrates the return advective flow to be induced as the two vortices "A" and "B" one above another. The upper vortex "A" with $\psi > 0$ revolves clockwise while the lower one "B" with $\psi < 0$ revolves counterclockwise. The vortex "A" is induced in the mantle wedge partially by subducting slab and to a lesser extent by convective mechanism as the latter cannot be completely excluded since the Rayleigh number $Ra$ is in the denominator in (2). The density of streamlines in Fig. 3 corresponds to the velocity of over ~ 1 (m/yr) in convective vortices (computed according to (4) with $Ra = 5.55\times10^8$). It should be noted that an unperturbed mantle wedge flow induced by the subduction of Arabian plate consists of the two flows "A" and "B" in Figs. 3(1) and 4(1) located one above another

only in the case of non-Newtonian rheology, and it is that in this case the localized zone of friction arises in which the subducting slab interacts with the counter-flowing material of vortex "A".

There the dissipative heating is high which generates the upwelling convective flow shown by vector $q$ in Figs. 3(4) and 4(4). Except for a heat this flow transports to the Earth's surface magmatic melts containing metallic ores of different geochemical composition. Depending on the presence of different chemical components in a subduction zone and its thermo-mechanical parameters different kind of ore-deposits may be formed, e.g. iron, copper or some other metals deposits. This is schematically outlined in a vertical cross-section of subduction zone in Fig. 5.

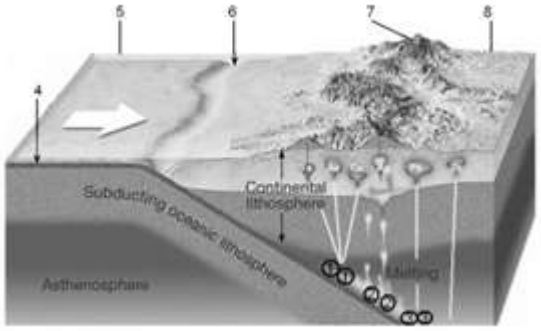


Fig. 5 Section diagram showing the appropriateness of distribution of metal provinces above the zones encompassing convective vortices in the zones of lithosphere plate subduction. 1, 2, 3 is the system of several pairs of thermo-mechanical convective vortices [12], facilitating the upwelling of alkali-lime magmas (containing metalized ores) to the upper layers of the Earth's crust; 4 – oceanic crust; 5 – Arabian suboceanic plate; 6 – trench; 7 – volcanic arc; 8 – Eurasian continental crust with the interaction of alkali-lime magmas (containing metalized ores).

In the eastern (Pakistani) block of AEZSLP the anomalous surface heat flux is somewhat lower than in the western segment because the water content in the porous rocks of mantle is enlarged and, according to our model, amounts to 1.48 wt.%, while the energy of activation there is by ~ 40 (kJ/mol) less as compared to that in the western segment. It is considered generally accepted that the energy of activation of the constituting rocks diminishes with growing medium "humidity", although there are no formulae for mathematical dependence of activational energy on water concentration. The model presented here shows the extent to which an anomalous surface heat flux allows estimating the diminution of the energy of activation with the growing water content in a given region. Finally, our modeling allows solving the inverse gravity problem, viz. to use the satellite Bouguer anomaly gravity data [6] to estimate the mean density $\rho_m \approx 3.4\times10^3$ (kg/m$^3$) of rocks in convective heterogeneity shown in Fig. 4(4). For this purpose the modeled values of depth of the upper boundary ($h_u \approx 300$ km), lower boundary ($h_b \approx 400$ km) and mean depth ($h_m \approx 350$ km) of convective heterogeneity, as well as its horizontal extent $2L \approx 400$ km (i.e. the convective cell horizontal dimension) were used. Comparing obtained density $\rho_m \approx 3.4\times10^3$ (kg/m$^3$) with the densities of different chemical complexes [12] permits to arrive at a conclusion that the prevailing composition of magmatic complexes in the convective heterogeneity under investigation possibly is close in density with erupted plutonic rocks like eclogite, which may contain considerable amounts of the copper-porphyry ores.

## VI. Conclusions

Modeling the geo-thermo-mechanical state of mantle wedge in the zone of subduction of Arabian suboceanic plate under Eurasian continental plate yields a convective instability to take place in the form of a single convective cell of the size of ~ 200 km in the case of non-Newtonian rheology and subducting velocity of 19 (mm/yr) characteristic of subduction in the western segment. The convection cell dimension and its localization do correspond exactly to the 2D breadth and geographical location of surface heat flux anomaly located at ~ 33ºN in the rear of Iranian block of subduction zone. Modeled ascending 2D convective flow in the rear of the eastem (Pakistani) block of subduction zone is shifted by ~ $10^2$ km landward in comparison to the western segment in excellent agreement with the localization of observed heat flux anomaly at ~ 34ºN. The heat flux diminution in the eastem part is shown to be due to the enlarged water content and lowered energy of activation because of more effective water withdrawal from subducting slab into the mantle wedge in the case of stick-slip subduction regime and "shaking" in the course of earthquakes. Convective flow ascending from the mantle wedge to the Earth's surface can transport lime-alkali magmas with a considerable amount of eclogite containing chemical metallic complexes (with Cu, Au, Ag etc.) and favor origination of the copper metal province in the south of Iran in the regions of enlarged heat flux anomaly correspondingly with the theoretical investigations [1], [2], [3].

## References

[1] R. H. Sillitoe, Relation of metal provinces in Western America to subduction of oceanic lithosphere. Bull. Geological Society of America, 1972, 83: 813-818. DOI: 10.1130/0016-7606(1972)83[813:rompiw]2.0.co;2.

[2] H. L. Barnes (Ed.), Geochemistry of hydrothermal ores deposits. 3rd ed. New York: John Wiley & Sons. Inc., 1997, 972 p.

[3] W. J. Morgan, Rises, trenches, great faults and crustal blocks. Journal of Geophysical Research. 1968, 73(6): 1959-1982. Available: URL: http://www.geologie.ens.rf

[4] M. Heidarzadeh, M. D. Pirooz, N. H. Zaker, A. C. Yalciner, C. E. Synolakis, Evaluating tsunami hazard in the Northwestern Indian Ocean. Pure and Applied Geophysics, 2008, 167: 2045-2058. DOI: 10.1007/s00024-008-0415-8.

[5] IHCF. Global Heat Flow Database of the International Heat Flow Commission. 2012. URL: https://ihfc-iugg.org/prod-ucts/global-heat-flow-database/data.

[6] Gravity anomaly map of Asia. Scale 1:9000000. New York: Pablished by the Aeronautical Chart and Information Center U.S. Air Force. 1971, 4 p.

[7] N. Mousavi, A. V. Ebrahimzadeh, 3D Surface Heat Flow, Low-Temperature Basins and Curie Point Depth of the Iranian Plateau: Hydrocarbon Reservoirs and Iron Deposits. Journal of the Earth and Space Physics, 2023, 48(4):137-150. DOI:10.22059/jesphys.2023.348000.1007453.

[8] G. Schubert, D. L. Turcotte, P. Olson, Mantle Convection in the Earth and Planets. New York: Cambridge University Press, 2001, 940 p. DOI:10.1017/CBO9780511612879.

[9] M. Billen, G. Hirth, Newtonian versus non-Newtonian Upper Mantle Viscosity: Implications for Subduction Initiation . Geophys. Res. Lett, 2005, 32: (L19304). DOI:10.1029/2005GL023458.
[10] V. P. Trubitsyn, Rheology of the mantle and tectonics of oceanic lithospheric plates. Physics of the Earth, 2012, 6: 3-22. (in Russ.).
[11] V. P. Trubitsyn, A. P. Trubitsyn, Numerical model of the formation of a set of lithospheric plates and their passage through the boundary of 660 km. Physics of the Earth, 2014, 6: 138-147. (in Russ.).
[12] M. H. P. Bott, The interior of the Earth. London: Edward Arnold, 1971, 370 p.

Date of submission of the article to the journal 01.09.2025
Sergey Gavrilov – Schmidt Institute of Physics of the Earth (e-mail: gavrilov@ifz.ru)
Andrey Kharitonov – Pushkov Institute of Terrestrial Magnetism, Ionosphere and Radio Wave Propagation of Russian Academy of Sciences (e-mail: haritonov-magnit@yandex.ru)